

# Spectral Splitting of Optical Pulses Inside a Dispersive Medium at a Temporal Boundary

Brent W. Plansinis, William R. Donaldson, *Member, IEEE*, and Govind P. Agrawal, *Fellow, IEEE*

**Abstract**—We show numerically that the spectrum of an optical pulse splits into multiple, widely separated, spectral bands when it arrives at a temporal boundary across which the refractive index suddenly changes. At the same time, the pulse breaks into several temporally separated pulses traveling at different speeds. The number of such pulses depends on the dispersive properties of the medium. We study the effect of second- and third-order dispersion in detail but also briefly consider the impact of other higher order terms. A temporal waveguide formed with two temporal boundaries can reflect the temporally separated pulses again and again, increasing the number of pulses trapped within the temporal waveguide.

**Index Terms**—Dispersive propagation, nonlinear optics, optical frequency conversion, ultrafast optics.

## I. INTRODUCTION

REFLECTION and refraction of light at a spatial boundary and Snell's laws that describe them have been understood for centuries and are thoroughly discussed in physics textbooks [1], [2]. Recently there has been a growing interest in the temporal analog of reflection and refraction, where an optical pulse arrives at a temporal boundary across which the refractive index changes suddenly in time [3]–[6]. The earliest works were focused on photon acceleration in plasmas [7], [8]. More recently, temporal reflection has been explored as analogs for gravity and Hawking radiation [9]–[13], as well as for dispersive waves scattering off of solitons [14]–[18]. Recently we showed that by using separated temporal boundaries, a temporal analog of optical waveguides can be created to confine an optical pulse between the two boundaries [19]. This effect has also been studied using two solitons that produce temporal boundaries through the nonlinear phenomenon cross-phase modulation (XPM) [20]–[25].

Manuscript received August 31, 2016; revised October 24, 2016; accepted October 27, 2016. Date of publication November 7, 2016; date of current version November 21, 2016. This work was supported in part by the Department of Energy National Nuclear Security Administration under Award DE-NA0001944, in part by the University of Rochester, in part by the New York State Energy Research and Development Authority, and in part by the National Science Foundation under Award ECCS-1505636.

B. W. Plansinis is with the Institute of Optics, University of Rochester, Rochester, NY 14627 USA, and also with the Laboratory for Laser Energetics, University of Rochester, Rochester, NY 14623-1299 USA (e-mail: bplansin@ur.rochester.edu).

W. R. Donaldson is with the Laboratory for Laser Energetics, University of Rochester, Rochester, NY 14623-1299 USA (e-mail: billd@lle.rochester.edu).

G. P. Agrawal is with the Laboratory for Laser Energetics, University of Rochester, Rochester, NY 14623-1299 USA, and also with the Institute of Optics, University of Rochester, Rochester, NY 14627 USA (e-mail: gpa@optics.rochester.edu).

Color versions of one or more of the figures in this paper are available online at <http://ieeexplore.ieee.org>.

Digital Object Identifier 10.1109/JQE.2016.2626081

An essential gradient for temporal reflection to occur is the group-velocity dispersion (GVD) of the medium in which an optical pulse approaches the temporal boundary [6]. However, to the best of our knowledge, the effects of higher-order dispersion have attracted little attention, apart from how it can shift the frequency of the reflected and refracted pulses. Since most practical media are likely to exhibit higher-order dispersive effects, in this paper we describe how they can lead to the formation of multiple pulses with widely separated spectral bands at a single temporal boundary.

The paper is organized as follows. In Sect. II we review the case where higher-order dispersion can be ignored and derive the temporal analogs of Snell's laws that predict the spectral shifts experienced by the “reflected” and “transmitted” pulses. In Sect. III we focus on the effects of third-order dispersion and briefly discuss the impact of even higher-order dispersion terms in Sect. IV. The effects of higher-order dispersion on temporal waveguides are discussed in Sect. V. The main results are summarized in Sect. VI.

## II. TEMPORAL REFLECTION AND REFRACTION

We consider an optical pulse in the form of a plane wave propagating inside a medium with a dispersion relation given by  $\beta(\omega) = n(\omega)\omega/c$ , where  $n(\omega)$  is the refractive index at frequency  $\omega$ . For a pulse containing multiple optical cycles, we can expand  $\beta(\omega)$  around a reference frequency  $\omega_0$  in a Taylor series as

$$\beta(\omega) = \beta_0 + \beta_1(\omega - \omega_0) + \frac{\beta_2}{2}(\omega - \omega_0)^2 + \frac{\beta_3}{6}(\omega - \omega_0)^3 + \dots, \quad (1)$$

where  $\beta_m = (d^m \beta / d\omega^m)_{\omega=\omega_0}$  are the dispersion parameters. Physically,  $\beta_1$  is the inverse of the group velocity,  $\beta_2$  is the GVD parameter, and  $\beta_3$  governs third-order dispersion (TOD). In this section we include only the GVD effects and neglect the TOD and higher-order terms in Eq. (1).

In general, the refractive-index boundary can be moving, so we work in a moving reference frame in which the temporal boundary is stationary. For a boundary moving at speed  $v_B$ , we can use the coordinate transform  $t = T - z/v_B$ , where  $T$  is the time in the laboratory frame. The dispersion relation then becomes [6]

$$\beta'(t) = \beta_0 + \Delta\beta_1(\omega - \omega_0) + \frac{\beta_2}{2}(\omega - \omega_0)^2 + \beta_B(t). \quad (2)$$

where  $\Delta\beta_1 = \beta_1 - 1/v_B$  is a measure of the relative speed of pulse's frequency component  $\omega$  relative to the boundary, and

$\beta_B(t) = k_0 \Delta n(t)$  is the change in the propagation constant caused by the time-dependent index change  $\Delta n(t)$ . The velocity of the temporal boundary should be chosen so that it is close to the group velocity of the optical pulse. For typical silica-based fibers with a group index  $n_g \approx 1.46$ , the temporal boundary should have a velocity close to  $v_B = 2 \times 10^8$  m/s. We have also assumed that terms higher than second order are negligible for the spectral range of interest and can be ignored. For a temporal boundary located at  $t = T_B$ , we assume that  $\beta_B$  takes the form of a step function. Fundamentally,  $\beta_B$  can have any value before or after the boundary, but we assume that  $\beta_B = 0$  for  $t < T_B$  and  $\beta_B$  is finite for  $t > T_B$  when  $T_B > 0$ . If  $T_B < 0$ , we reverse this such that  $\beta_B$  is finite for  $t < T_B$  and  $\beta_B = 0$  for  $t > T_B$ .

We can further simplify our discussion by choosing our reference frequency such that the group velocity at that frequency matches the speed of the temporal boundary. In this case  $\Delta\beta_1 = 0$ , and the dispersion relation becomes

$$\beta'(\Delta\omega) = \beta_0 + \frac{\beta_2}{2} \Delta\omega^2 + \beta_B(t), \quad (3)$$

where  $\Delta\omega$  is the frequency offset from the new reference frequency ( $\omega_0$ ).

Using Maxwell's equations with the simplified dispersion relation in Eq. (3) and making the slowly varying envelope approximation, we obtain the following time-domain equation:

$$\frac{\partial A}{\partial z} + \frac{i\beta_2}{2} \frac{\partial^2 A}{\partial t^2} = i\beta_B(t)A, \quad (4)$$

where  $A(z, t)$  is the pulse envelope at a distance  $z$ . We solve Eq. (4) numerically using the standard split-step Fourier method [26]. The temporal and spectral evolutions of a Gaussian pulse whose carrier frequency is shifted from  $\omega_0$  by  $\Delta\omega_i$  is shown in Fig. 1 using the input field in the form

$$A(0, t) = \exp[-t^2/(2T_0^2)] \exp(i\Delta\omega_i t), \quad (5)$$

with the parameter values  $T_0 = 1.5$  ps,  $T_B = 5$  ps,  $\Delta\omega_i = 10^{13}$  s<sup>-1</sup>,  $\beta_2 = 0.05$  ps<sup>2</sup>/m, and  $\beta_B = 2$  m<sup>-1</sup>. This value of  $\beta_B$  corresponds to a refractive index change of less than  $10^{-6}$  at a wavelength of  $1 \mu\text{m}$ .

The temporal evolution seen in Fig. 1(a) is analogous to an optical beam undergoing reflection and refraction at a spatial boundary in the sense that a part of the pulse energy appears to reflect backward in time. However, we should stress that both parts of the pulse are propagating forward; the reflected pulse travels faster than the temporal boundary and only appears to move backward in time in the reference frame that is moving with the temporal boundary. The reason for this increase in speed is apparent from the spectral evolution in Fig. 1(b), which shows that the spectrum shifts toward the red side and splits into two distinct spectral bands that travel at different speeds because of the GVD. These spectral shifts occur because a temporal boundary breaks translational symmetry in time. As a result, photon momentum (or  $\beta'$ ) must be conserved while photon energy (or  $\omega$ ) may change. Mathematically, momentum is conserved by finding solutions

$$\beta'(\Delta\omega, t) = \beta'(\Delta\omega_i, t = 0), \quad (6)$$

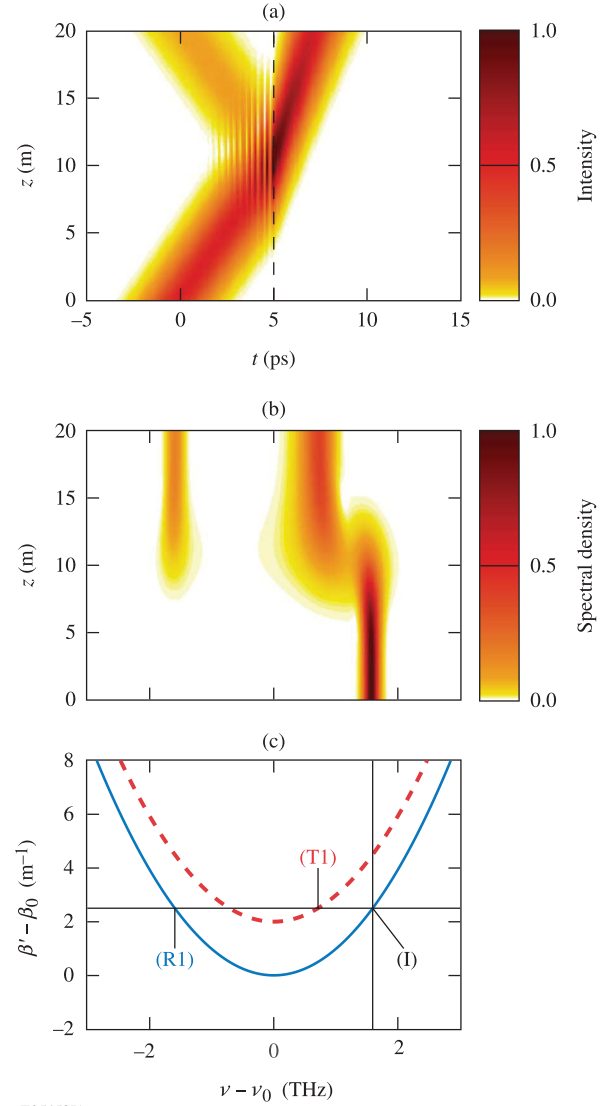


Fig. 1. Evolution of (a) intensity and (b) spectrum as a Gaussian pulse crosses a temporal boundary (dashed black line) with  $\beta_B = 2$  m<sup>-1</sup>. (c) Dispersion curves for  $t < T_B$  (solid blue) and  $t > T_B$  (dashed red).

where the right side is the initial propagation constant at  $\Delta\omega_i$ . Figure 1(c) shows a plot of the dispersion curve for  $t < T_B$  in solid blue and for  $t > T_B$  in dashed red. Note that the red curve is the same as the blue curve if it were shifted up by  $\beta_B$ . As marked in Fig. 1(c), (I) corresponds to the initial pulse frequency, (R1) is the reflected pulse frequency, and (T1) is the transmitted pulse frequency. The unlabeled solution to Eq. 6 on the transmitted curve is not a valid solution because the relative group velocity at that frequency would not carry the transmitted pulse across the boundary into the  $t > T_B$  region [6]. The requirement that the sign of the relative group velocity must take the pulse into the correct temporal region is referred to as the group-velocity restriction.

We can easily solve Eq. (6) to find analytic expressions for the reflected and transmitted frequencies as

$$\Delta\omega_r = -\Delta\omega_i, \quad (7)$$

$$\Delta\omega_t = \Delta\omega_i \sqrt{1 - \frac{2\beta_B\beta_2}{\Delta\beta_1^2}}, \quad (8)$$

where  $\Delta\beta_1 = \beta_2\Delta\omega_i$  is now a measure of the speed of the incident pulse relative to the speed of the boundary. These equations are the temporal analogs to the laws of reflection and refraction. Examining Eq. (8), we find that the transmitted frequency becomes complex when  $\Delta\beta_1 < \sqrt{2\beta_B\beta_2}$ , which is not physical. When this condition is satisfied, the transmitted pulse no longer propagates and a temporal analog of total internal reflection (TIR) occurs [6].

### III. THIRD-ORDER DISPERSION EFFECTS

We now consider the case where the effects of TOD are large enough that we can no longer ignore it in the Taylor expansion of  $\beta(\omega)$ . The dispersion relation then becomes

$$\beta'(\Delta\omega) = \beta_0 + \frac{\beta_2}{2}\Delta\omega^2 + \frac{\beta_3}{6}\Delta\omega^3 + \beta_B(t), \quad (9)$$

where we again choose a reference frequency with a group velocity that matches the speed of the temporal boundary.

As before, when the pulse crosses the temporal boundary it shifts its frequency such that the momentum is conserved in the moving frame. To find these frequencies, we again find the solutions to Eq. (6) and apply the group-velocity restriction. However, we now use Eq. (9) for the dispersion relation, which allows for up to three solutions for both the reflected ( $t < T_B$ ) and transmitted ( $t > T_B$ ) curves. Although the roots of a cubic polynomial are well known, in general they do not lead to simple relations such as those given in Eqs. (7) and (8). Moreover, there can be at most two reflected or two transmitted frequencies because of the group-velocity restriction (slope of the dispersion curve). This is because the cubic polynomial has two regions that have a slope of one sign, and one region between these two that has a slope of the opposite sign.

We first examine the case where two transmitted pulses can form, as shown in Fig. 2. For this simulation, we used the same parameters as in Fig. 1, but chose  $\beta_3 = 4.5 \text{ ps}^3/\text{km}$  and  $\beta_B = 3 \text{ m}^{-1}$  to clearly resolve all pulses that form while crossing the temporal boundary. We see the incident pulse split into three pulses, forming one reflected pulse and two transmitted pulses. The two transmitted pulses travel at different speeds, separating as they travel further through the material.

Figure 2(b) shows that reflection and refraction are once again accompanied by shifting and splitting of the spectrum, but the spectrum now splits into three distinct spectral bands. Examining the dispersion curves in Fig. 2(c) we see that the two transmitted pulses correspond to bands centered (T1) at  $-5.3 \text{ THz}$  and (T2) at  $0.48 \text{ THz}$ , and the reflected pulse corresponds to the middle frequency (R1) at  $-2.5 \text{ THz}$ . The new transmitted pulse (T1) forms because the TOD term bends the dispersion curve back toward the initial value, creating two regions where the group-velocity restriction can be satisfied. We emphasize that both T1 or and T2 are always present regardless of how large  $\beta_B$  becomes or what sign it takes. Therefore, in this case temporal TIR cannot occur. However, if the magnitude of  $\beta_B$  is large, the amount of energy transferred to the transmitted pulse is very small, and the pulse is almost entirely reflected.

Examining the dispersion curve in Fig. 2(c), we see that if the initial pulse frequency were shifted further to the right

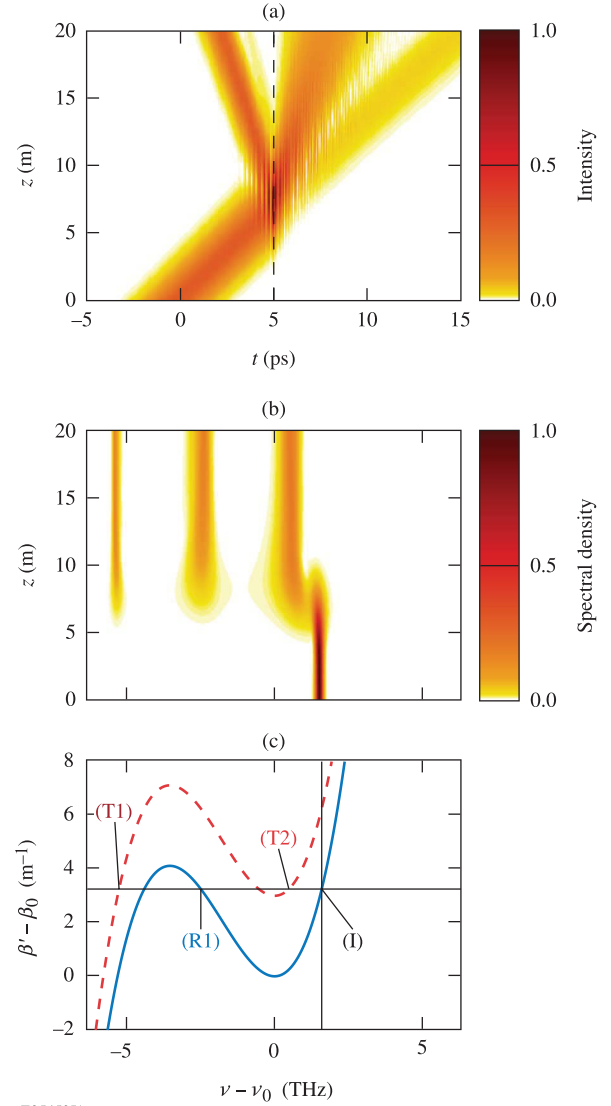
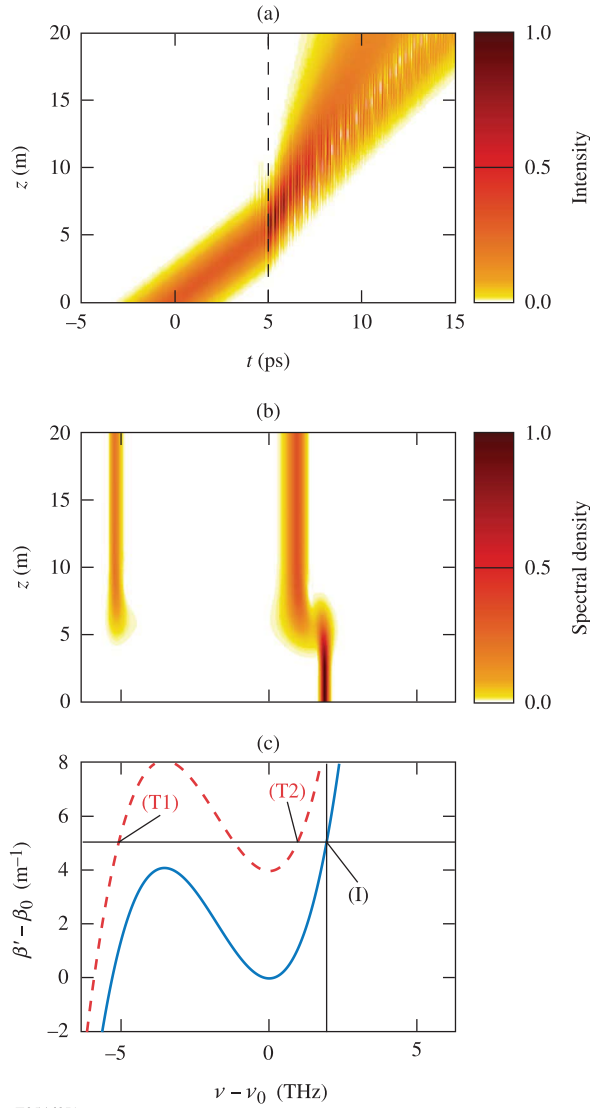


Fig. 2. (a) and (b) Same as Fig. 1 except that TOD is included. The presence of TOD allows for two transmitted frequencies. (c) Dispersion curves for  $t < T_B$  (solid blue) and  $t > T_B$  (dashed red).

there would eventually be no solution for the reflected pulse on the incident curve (solid blue) that satisfies momentum conservation. This situation is similar to the Brewster angle in the case of a spatial boundary. Figure 3 shows a simulation where we have kept all of the parameters the same as in Fig. 2, but increased the initial frequency shift to  $\Delta\omega_i/(2\pi) = 1.94 \text{ THz}$  and the index shift at the boundary to  $\beta_B = 4 \text{ m}^{-1}$ . As Fig. 3(a) and Fig.3(b) show, no reflected pulse is formed in this case since there is no valid solution in Fig. 3(c) on the blue curve where momentum conservation can be satisfied. Therefore, all of the pulse energy must be transferred to the transmitted frequencies, T1 and T2. If the magnitude of  $\beta_B$  were to be increased further, the root T2 would eventually no longer exist, and all of the pulse energy would be transferred to a single transmitted pulse at T1. If the sign of  $\beta_B$  were changed, the same situation would occur, but the initial pulse energy would be entirely transferred to point T2. The main point to note is that the presence of TOD modifies the

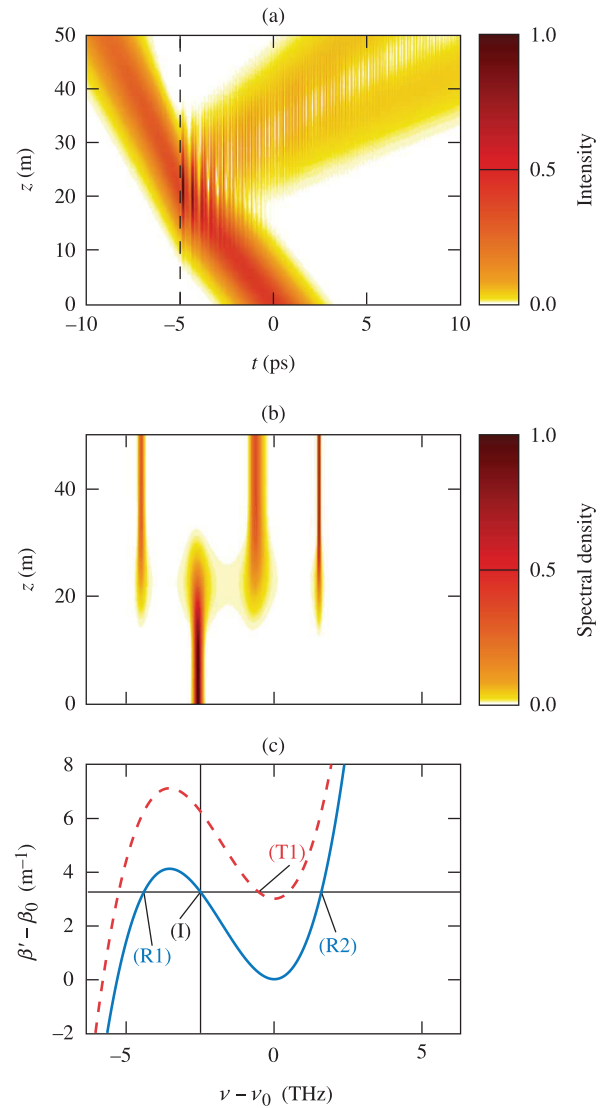


E25460J1

Fig. 3. (a) and (b) Same as Fig. 2 but the initial frequency shift has been increased to  $\Delta\omega_i/(2\pi) = 1.94$  THz. (c) Dispersion curves for  $t < T_B$  (solid blue) and  $t > T_B$  (dashed red).

dispersion curve so much that many novel and interesting scenarios can occur at a temporal boundary.

Another interesting case occurs when the initial pulse spectrum is located in the middle section of the dispersion curve, where the slope has the opposite sign from the two outer regions of the dispersion curve. In this configuration, we expect to see two reflected frequencies that satisfy both conservation of momentum and the group-velocity requirement. Figure 4 shows this situation using the same Gaussian pulse used in Fig. 2, but with an initial frequency shift of  $\Delta\omega_i/(2\pi) = -2.5$  THz. This frequency shift was chosen to match point (R1) in Fig. 2. Because the sign of the relative group velocity has changed (the dispersion slope is negative instead of positive), the pulse will move toward negative times. Recall that because we are in a reference frame moving with the boundary, this only means that the pulse is moving faster than the boundary. To account for this change in relative velocity, the temporal boundary must be moved to  $T_B = -5$  ps



E25461J1

Fig. 4. Evolution of (a) intensity and (b) spectrum for a Gaussian pulse in the presence of a temporal boundary (dashed black line) for  $\beta_B = 3 \text{ m}^{-1}$  and  $\Delta\omega_i/(2\pi) = -2.5$  THz. (c) Dispersion curves for  $t < T_B$  (solid blue) and  $t > T_B$  (dashed red).

with the shift of  $\beta_B$  occurring for  $t < -5$  ps so that the optical pulse would still cross the same boundary. In Fig. 4(a), the optical pulse crosses the boundary and once again splits into three pulses. This time only one pulse is transmitted, while two pulses are reflected with different speeds. Figures 4(b) and 4(c) show that this corresponds to three spectral bands at points R1 and R2 for the reflected pulses, and the point T1 for the transmitted pulse.

Unlike Figs. 2 and 3, the process in Fig. 4 allows for temporal TIR. Indeed, if the magnitude of  $\beta_B$  is increased, there will no longer be any T1 point that satisfies momentum conservation. More interestingly, the TIR condition can be reached even if  $\beta_B$  has the opposite sign, which would shift the dispersion curve down. This is different from the case where TOD is not present, where the TIR condition can only be met using a particular sign for  $\beta_B$  because there is a single global minimum ( $\beta_2 > 0$ ) or maximum ( $\beta_2 < 0$ ).

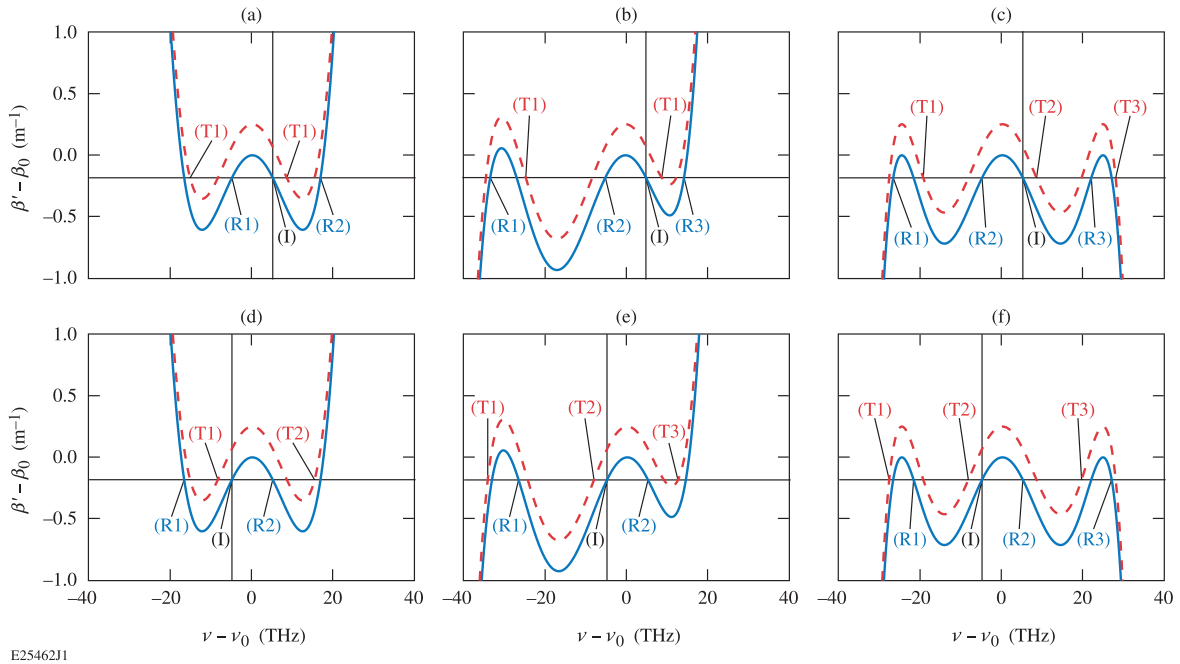


Fig. 5. Example dispersion curves for  $t < T_B$  (solid blue) and  $t > T_B$  (dashed red) when the highest-order dispersion term is [(a),(d)]  $\beta_4$ , [(b),(e)]  $\beta_5$ , and [(c),(f)]  $\beta_6$ . The top row shows an initial frequency with a positive slope, and the bottom row shows an initial frequency with a negative slope.

Finally, unlike the temporal reflection in Section II, the spectrum of the reflected pulse narrows or broadens depending on where the input pulse lies on the dispersion curve. This occurs because a pulse contains a range of frequencies, and the dispersion relation must be conserved at each of these frequencies. For a given input frequency, the range of values the dispersion relation ( $\beta'$ ) can take depends on the slope of the dispersion curve. For a fixed input pulse spectrum, a higher dispersion slope will cover a wider range of  $\beta'$  values. Therefore, if the slope of the dispersion curve is larger at the input frequency than at the reflected frequency, the reflected pulse will have a wider spectrum, as in Fig. 2. However, if the opposite is true, as in Fig. 4, the spectrum of the reflected pulse will be narrower.

#### IV. HIGHER-ORDER DISPERSION EFFECTS

If we continue to increase the number of dispersion terms in the Taylor expansion in Eq. (1), the number of possible solutions to Eq. (6) will increase for both the reflected and transmitted curves. As with the TOD simulations, not every solution to Eq. (6) is permitted because of the group-velocity restriction. However, based on conservation of momentum and the group-velocity restriction, we can find the maximum number of reflected, transmitted, and total pulses that can form as the pulse crosses the boundary.

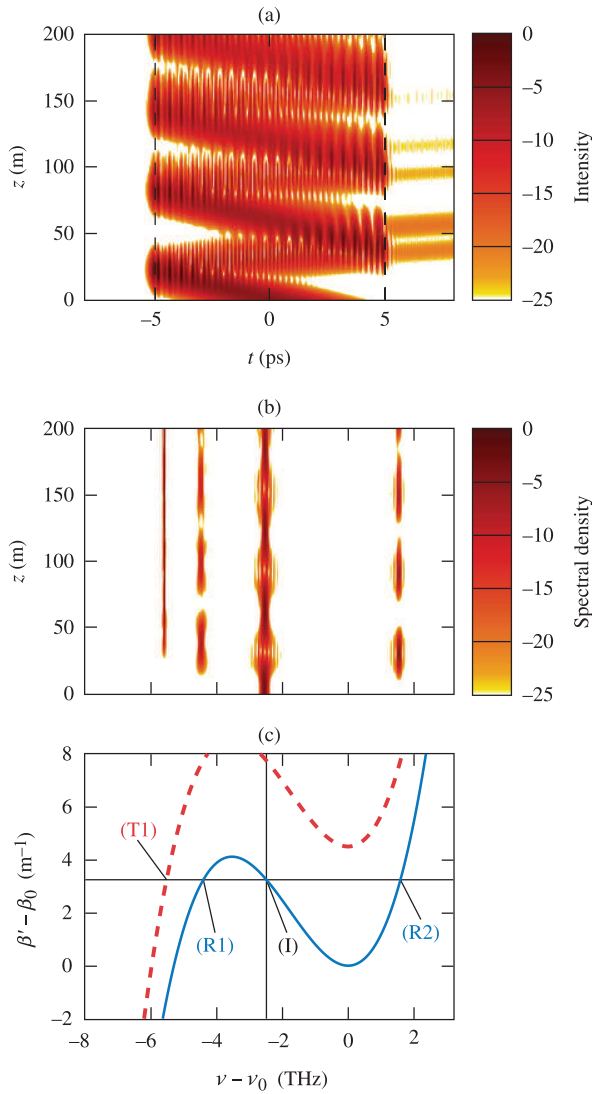
Figure 5 shows dispersion curves with  $\beta_B = 0.5$  ps/m,  $\beta_2 = -0.4$  ps<sup>2</sup>/m,  $\beta_4 = 4 \times 10^{-4}$  ps<sup>4</sup>/km, and [(a),(d)] no more higher-order terms, [(b),(e)]  $\beta_5 = 7 \times 10^{-6}$  ps<sup>5</sup>/km, and [(c),(f)]  $\beta_6 = 2.5 \times 10^{-7}$  ps<sup>6</sup>/km for two different initial frequencies. The  $\beta_2$  and  $\beta_4$  terms were chosen to match a commercially available photonic crystal fiber. The values for  $\beta_5$  and  $\beta_6$  do not correspond to this same fiber, but were

chosen such that all roots exist over the spectral region to better illustrate the effect of higher order dispersion. We see that the maximum number of pulses that can form at the temporal boundary is equal to the order of the polynomial. Explicitly, this means that  $\beta_4$  generates up to four pulses,  $\beta_5$  up to five pulses, and  $\beta_6$  up to six pulses. This makes sense because transmitted pulses will form at solutions to Eq. (6) that have a slope matching the sign of the input frequency, while the reflected pulses will form at the solutions with a slope of the opposite sign.

The number of either reflected or transmitted pulses depends not only on the number of dispersion terms but also on where the input pulse spectrum is located. In the case of even-order dispersion, half of the solutions represent reflected pulses and the other half transmitted pulses. The situation becomes more complex when the last term is odd. For example, when terms up to  $\beta_5$  are included, five pulses are formed at the boundary. As seen in Fig. 5, three of them are transmitted when  $\Delta\omega_i > 0$  but three of them are reflected when  $\Delta\omega_i < 0$ . Similar to the TOD case, this occurs because the fifth-order dispersion curve has three regions with a slope of one sign, and only two regions with a slope of the opposite sign. Note that these are all upper limits to the number of reflected and transmitted pulses. If different dispersion parameters, initial frequencies, or ( $\beta_B$  values are chosen, the number of pulses formed can decrease. We emphasize that even-order dispersion always allows for TIR to occur, regardless of the location of the initial pulse spectrum. This makes sense because even order polynomials have either a global maximum or a global minimum.

#### V. TEMPORAL WAVEGUIDES

If an optical pulse is placed between two temporal boundaries, the pulse can be trapped between the two boundaries,



E25463J1

Fig. 6. Evolution of (a) pulse shape and (b) spectrum in a temporal waveguide formed by two boundary (dashed black lines) in the same medium as Fig. 4 with  $\Delta\omega_i/(2\pi) = -2.5$  THz. Note that intensity and spectral density are now on a logarithmic scale to better show the transmitted pulses. (c) Dispersion curves inside (solid blue) and outside (dashed red) the waveguide.

forming a temporal analog of an optical waveguide [19]. When higher-order dispersion is negligible, these waveguides behave like spatial planar waveguides, including having a finite number of supported modes. In this section we consider the effects of higher-order dispersion on temporal waveguides. Here we focus at the effects of TOD only since this is the most dominant term in practice. The new features that arise in this case are also expected to occur when fourth- or fifth-order dispersion terms are included.

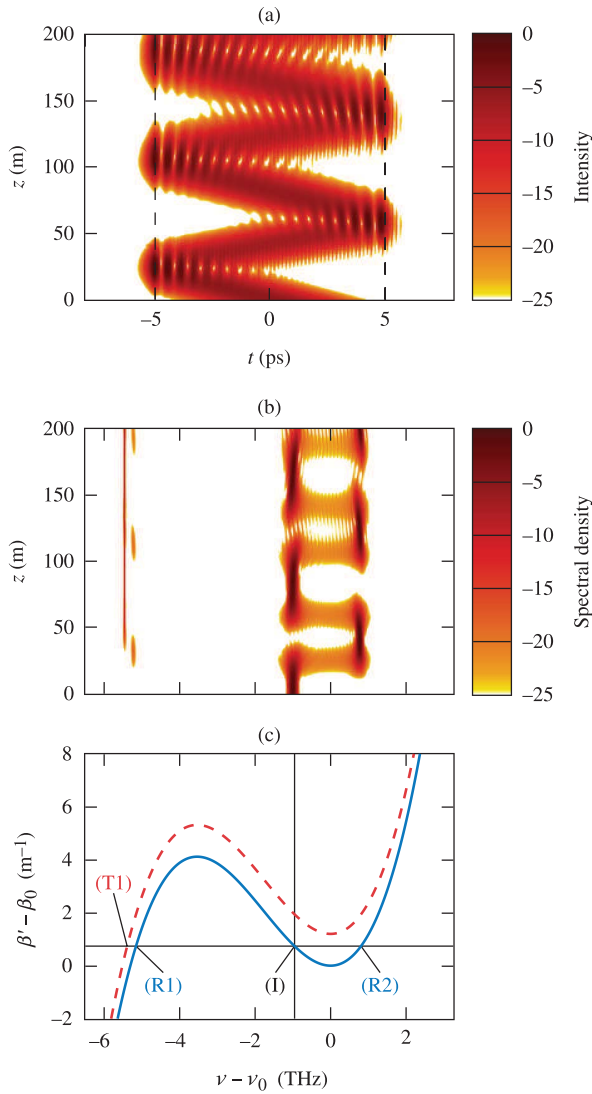
Figure 6 shows the propagation of a Gaussian pulse with  $T_0 = 2$  ps under conditions of Fig. 4 except that we now have two temporal boundaries located at  $t = \pm 5$  ps. The value of  $\beta_B$  was increased to  $4.5 \text{ m}^{-1}$  to remove the transmitted frequency near  $\nu = \nu_0$  and allow for the TIR condition to be satisfied at the input wavelength. As Figs. 6(a) and 6(b) show, the TIR condition holds when the pulse hits the first boundary

at  $t = -5$  ps, forming two reflected pulses (R1 and R2). These two pulses interfere with each other as they propagate, forming interference fringes. The reflected pulses travel with slightly different group velocities, and so they reach the second boundary at  $t = 5$  ps at different distances. When each of them hits the second boundary at  $t = 5$  ps, some energy is transmitted because the group-velocity restriction can now be satisfied since the slope of the dispersion curve at R1 and R2 is now positive allowing energy to transfer to T1. Because each of the reflected pulses hits the boundary at a different distance, two transmitted pulses form at the same frequency.

In addition to generating the transmitted pulses, both pulses also reflect off the boundary and travel back to the other boundary at  $t = -5$  ps. At this point, the process repeats itself, but because of the different distances at which the pulses reach the boundary there are two pulses at the initial frequency instead of one. After another round-trip through the waveguide, each of these two pulses will split into two more pulses. However, two of these new pulses will overlap in time, and so only three distinct pulses will be seen. This process can repeat as long as the pulses are trapped within the temporal waveguide, and the temporal waveguide will act as a pulse multiplier. For the simulations shown in Fig. 6, multiple pulses cannot be clearly distinguished because they overlap in time. By increasing the width of the waveguide, the reflected pulses will separate more in time before crossing the second boundary and forming two distinct pulses at the initial frequency.

A transmitted frequency will always exist for either the incident or reflected pulses regardless of the magnitude of  $\beta_B$ , so this loss cannot be avoided for a waveguide with TOD. However, the loss can be significantly reduced by working at frequencies near either the local maximum or local minimum, whichever is further from the transmitted frequency. For example, Fig. 7 shows the spectral and temporal evolutions when the initial pulse frequency is changed to  $\Delta\omega_i/(2\pi) = -0.96$  THz. In this case, much less energy is transferred to frequencies R1 and T1, and the behavior more closely resembles that of a waveguide without TOD. Although there are still interference fringes in the time domain, these fringes arise from the beating of the input frequency with the reflected frequency R2, rather than from the two reflected frequencies beating with one another.

When the temporal waveguide supports several modes, the frequency of the fundamental mode will occur near the local minimum of the dispersion curve, similar to that in Fig. 7. The mode shape can then be well-approximated by ignoring the higher-order dispersion terms, and little energy will be lost at the temporal boundaries. However, the higher-order modes will have a larger  $\Delta\omega$ , and will be more strongly affected by TOD. As a result, higher-order modes will lose more energy as transmitted pulses, as in Fig. 6. A short optical pulse with a large spectral bandwidth is likely to excite several modes when launched into such a waveguide. However, given a long enough propagation distance, only the fundamental mode would remain confined within the waveguide, with the other modes losing energy to the transmitted frequency.



E25464J1

Fig. 7. [(a),(b)] Same as Fig. 6 except that  $\Delta\omega_i/(2\pi) = -0.96$  THz and  $\beta_B = 1.2 \text{ m}^{-1}$ . Note that intensity and spectral density are now on a logarithmic scale to better show the transmitted and secondary reflected frequencies. (c) Dispersion curves inside (solid blue) and outside (dashed red) the waveguide.

## VI. CONCLUSIONS

We have shown through numerical simulations that the spectrum of an optical pulse splits into multiple, widely separated, spectral bands when it arrives at a temporal boundary across which refractive index suddenly changes. At the same time, the pulse breaks into several temporally separated pulses traveling at different speeds. The number of such pulses depends on the dispersive properties of the medium. In the case of a parabolic dispersion curve, the second-order dispersion governed by  $\beta_2$  splits the input pulse into two pulses with widely separated spectra that represent the temporal analogs of reflection and refraction at a spatial boundary [6]. The inclusion of higher-order dispersion makes it possible to form multiple reflected and transmitted pulses at a temporal boundary with widely separated spectral bands. More specifically, in the case of third-order dispersion, the pulse splits into three pulses, where the third one may correspond to either a reflected or a

transmitted pulse depending on the wavelength of the input pulse. Furthermore, if the input wavelength is far enough from a wavelength where the dispersion curve exhibits an extremum, it is possible that only two transmitted pulses are formed without any temporal reflection. Conversely, if the input wavelength is close to a local maximum or minimum, the amount of energy transferred to the third pulse becomes negligible. The behavior of the pulse is then accurately modeled by neglecting the third-order dispersion term.

We also discussed the situation in which a temporal waveguide is formed by using two temporal boundaries. The role of second-order dispersion for such waveguides is already known [19]. In this paper we found the the third-order dispersion introduces several new features. First, it is possible to produce two reflected pulses with widely separated spectra at one of the boundaries. These two pulses separate in time before arriving at the second boundary, leading to additional pulses. This process cascades each time the pulses bounce through the waveguide, allowing the temporal waveguide to act as a pulse multiplier. Unfortunately, undesirable transmitted pulses also form, representing loss of energy from a temporal waveguide. However, the energy loss can be minimized by suitably optimizing the input wavelength.

From a practical perspective, the importance of higher-order terms depends not only on the width of input pulses but also how far the input wavelength is from a maximum or minimum of the dispersion curve of the material. For example for silica fibers used in the telecom region near 1550 nm, the effects of  $\beta_2$  dominate and no more than two pulses will form at a temporal boundary because dispersion terms higher than second order will simply shift the frequencies of the reflected and transmitted pulses. However, if the pulse spectrum is located near the zero dispersion wavelength of the fiber, either by choosing the proper wavelength or by employing special dispersion-shifted fibers, the TOD term becomes significant and up to three pulses can form as in Figs. 2 and 4. Furthermore, microstructured and photonic crystal fibers make it possible to tailor the dispersion and can be designed with dispersion curves that exhibit more than one zero-dispersion wavelength. Such fibers could allow the formation of multiple pulses with widely separated spectral bands ( $> 50$  nm) if a suitable temporal boundary can be produced using a nonlinear effect such as cross-phase modulation.

## ACKNOWLEDGMENT

This report was prepared as an account of work sponsored by an agency of the U.S. Government. Neither the U.S. Government nor any agency thereof, nor any of their employees, makes any warranty, express or implied, or assumes any legal liability or responsibility for the accuracy, completeness, or usefulness of any information, apparatus, product, or process disclosed, or represents that its use would not infringe privately owned rights. Reference herein to any specific commercial product, process, or service by trade name, trademark, manufacturer, or otherwise does not necessarily constitute or imply its endorsement, recommendation, or favoring by the U.S. Government or any agency thereof.

The views and opinions of authors expressed herein do not necessarily state or reflect those of the U.S. Government or any agency thereof.

## REFERENCES

- [1] M. Born and E. Wolf, *Principles of Optics: Electromagnetic Theory of Propagation, Interference, and Diffraction of Light*, 7th ed. Cambridge, U.K.: Cambridge Univ. Press, Oct. 1999.
- [2] B. E. A. Saleh and M. C. Teich, *Fundamentals Photonics*, 2nd ed. Hoboken, NJ, USA: Wiley, 2007.
- [3] J. T. Mendonça and P. K. Shukla, "Time refraction and time reflection: Two basic concepts," *Phys. Scripta*, vol. 65, no. 2, pp. 160–163, Aug. 2002.
- [4] F. Biancalana, A. Amann, A. V. Uskov, and E. P. O'Reilly, "Dynamics of light propagation in spatiotemporal dielectric structures," *Phys. Rev. E*, vol. 75, no. 4, p. 046607, Apr. 2007.
- [5] K. A. Lurie, "An introduction to the mathematical theory of dynamic materials," in *Advances in Mechanics and Mathematics*, vol. 15. New York, NY, USA: Springer, 2007.
- [6] B. W. Plansinis, W. R. Donaldson, and G. P. Agrawal, "What is the temporal analog of reflection and refraction of optical beams?" *Phys. Rev. Lett.*, vol. 115, no. 18, p. 183901, Oct. 2015.
- [7] S. C. Wilks, J. M. Dawson, W. B. Mori, T. Katsouleas, and M. E. Jones, "Photon accelerator," *Phys. Rev. Lett.*, vol. 62, no. 22, pp. 2600–2603, May 1989.
- [8] J. T. Mendonça, *Theory of Photon Acceleration (Plasma Physics)*. Bristol, England: Institute of Physics, 2001.
- [9] T. G. Philbin, C. Kuklewicz, S. J. Robertson, S. Hill, F. König, and U. Leonhardt, "Fiber-optical analog of the event horizon," *Science*, vol. 319, no. 5868, pp. 1367–1370, Mar. 2008.
- [10] F. Belgiorno *et al.*, "Hawking radiation from ultrashort laser pulse filaments," *Phys. Rev. Lett.*, vol. 105, no. 20, p. 203901, Nov. 2010.
- [11] E. Rubino *et al.*, "Experimental evidence of analogue Hawking radiation from ultrashort laser pulse filaments," *New J. Phys.*, vol. 13, no. 8, p. 085005, 2011.
- [12] D. Faccio, "Laser pulse analogues for gravity and analogue Hawking radiation," *Contemp. Phys.*, vol. 53, no. 2, pp. 97–112, Dec. 2012.
- [13] D. Faccio, T. Arane, M. Lamperti, and U. Leonhardt, "Optical black hole lasers," *Class. Quantum Grav.*, vol. 29, no. 22, p. 224009, Oct. 2012.
- [14] A. V. Gorbach and D. V. Skryabin, "Bouncing of a dispersive pulse on an accelerating soliton and stepwise frequency conversion in optical fibers," *Opt. Exp.*, vol. 15, no. 22, pp. 14560–14565, Oct. 2007.
- [15] S. Robertson and U. Leonhardt, "Frequency shifting at fiber-optical event horizons: The effect of Raman deceleration," *Phys. Rev. A*, vol. 81, no. 6, p. 063835, Jun. 2010.
- [16] A. Demircan, S. Amiranashvili, and G. Steinmeyer, "Controlling light by light with an optical event horizon," *Phys. Rev. Lett.*, vol. 106, no. 16, p. 163901, Apr. 2011.
- [17] E. Rubino *et al.*, "Soliton-induced relativistic-scattering and amplification," *Sci. Rep.*, vol. 2, Dec. 2012, Art. no. 932.
- [18] L. Tartara, "Frequency shifting of femtosecond pulses by reflection at solitons," *IEEE J. Quantum Electron.*, vol. 48, no. 11, pp. 1439–1442, Nov. 2012.
- [19] B. W. Plansinis, W. R. Donaldson, and G. P. Agrawal, "Temporal waveguides for optical pulses," *J. Opt. Soc. Amer. B*, vol. 33, no. 6, pp. 1112–1119, Jun. 2016.
- [20] A. Shipulin, G. Onishchukov, and B. A. Malomed, "Suppression of soliton jitter by a copropagating support structure," *J. Opt. Soc. Amer. B*, vol. 14, no. 12, pp. 3393–3402, Dec. 1997.
- [21] R. Driben, A. V. Yulin, A. Efimov, and B. A. Malomed, "Trapping of light in solitonic cavities and its role in the supercontinuum generation," *Opt. Exp.*, vol. 21, no. 16, pp. 19091–19096, Aug. 2013.
- [22] A. Demircan, S. Amiranashvili, C. Brée, U. Morgner, and G. Steinmeyer, "Supercontinuum generation by multiple scatterings at a group velocity horizon," *Opt. Exp.*, vol. 22, no. 4, pp. 3866–3879, Feb. 2014.
- [23] J. Steinhauer, "Observation of self-amplifying Hawking radiation in an analogue black-hole laser," *Nature Phys.*, vol. 10, no. 11, pp. 864–869, Nov. 2014.
- [24] S. F. Wang, A. Mussot, M. Conforti, X. L. Zeng, and A. Kudlinski, "Bouncing of a dispersive wave in a solitonic cage," *Opt. Lett.*, vol. 40, no. 14, pp. 3320–3323, Jul. 2015.
- [25] Z. Deng, X. Fu, J. Liu, C. Zhao, and S. Wen, "Trapping and controlling the dispersive wave within a solitonic well," *Opt. Exp.*, vol. 24, no. 10, pp. 10302–10312, May 2016.
- [26] G. P. Agrawal, *Nonlinear Fiber Optics*, 5th ed. Amsterdam, The Netherlands: Elsevier, 2013.



**Brent W. Plansinis** received the B.S. degree (Hons.) in physics from Pennsylvania State University, The Behrend College, in 2011. He is currently pursuing the Ph.D. degree in optics from the Institute of Optics, University of Rochester with a focus on the applications of the space-time analogy.

Since 2012, he has been with the Laboratory for Laser Energetics to develop a method for single-shot detection of picosecond pulses using a lithium niobate phase modulator as a time-lens. His research interests include nonlinear effects in dispersive media, temporal analogs of spatial systems, short pulse interactions with temporal refractive index boundaries, and the measurement of ultrafast pulses.

Mr. Plansinis is a member of the Optical Society of America and SPIE student chapters.



**William R. Donaldson** (M'80) received the B.S. degree in physics and mathematics from Carnegie-Mellon University in 1976 with University Honors, and the Ph.D. degree in electrical engineering from Cornell University in 1984 with the focus on the use of organic crystals for an optical parametric oscillator.

He joined the Laboratory for Laser Energetics, University of Rochester as a Research Associate in 1984. In 1986, he was promoted to a Staff Scientist. In 2009, he was appointed as a Professor of Electrical and Computer Engineering with the Electrical and Computer Engineering Department, University of Rochester. He holds four patents. He has authored or co-authored several scientific papers. His research interests include the physics of photoconductive switches, streak-camera development, the optical response of high temperature superconductors, optical semiconductor diagnostics, and the fluorescence of biological molecules.

Dr. Donaldson is a member of the American Physical Society, the Optical Society of America, and the Institute of Electrical and Electronic Engineers.



**Govind P. Agrawal** (M'81–F'96) received the B.S. degree from the University of Lucknow in 1969 and the M.S. and Ph.D. degrees from the IIT Delhi, New Delhi, in 1971 and 1974, respectively.

He held various positions with École Polytechnique, France, The City University of New York, and Bell Laboratories, Murray Hill, NJ, USA. He joined the Faculty of the Institute of Optics, University of Rochester, in 1989, where he is currently the James C. Wyant Professor of Optics. He has authored or co-authored over 400 research papers and eight books. His books *Nonlinear Fiber Optics* (Academic Press, 5th ed., 2013) and *Fiber-Optic Communication Systems* (Wiley, 4th ed., 2010) are used worldwide for research and teaching. His research interests focus on optical communications, nonlinear optics, and laser physics. In 2012, the IEEE Photonics Society honored him with its prestigious Quantum Electronics Award. He was a recipient of the 2013 William H. Riker University Award for Excellence in Graduate Teaching. He became the Editor-in-Chief of the *Advances in Optics and Photonics Journal* in 2014 and was awarded the Esther Hoffman Beller Medal in 2015. From 2009 to 2010 he chaired the Publication Council and served on the Board of Directors of OSA. He is involved with both the IEEE and the Optical Society (OSA) and has helped them with journal publishing and conference organization.

Dr. Agrawal is a fellow of OSA. He is also a Life Fellow of the Optical Society of India.